

# Theoretical calculations and experimental measurements of the structure of $Ti_5Si_3$ with interstitial additions

J.J. Williams<sup>a,b</sup>, Y.Y. Ye<sup>c</sup>, M.J. Kramer<sup>a,b,\*</sup>, K.M. Ho<sup>a</sup>, L. Hong<sup>c</sup>,  
C.L. Fu<sup>d</sup>, S.K. Malik<sup>e,f</sup>

<sup>a</sup>Ames Laboratory, US Department of Energy, Ames, IA 50011, USA

<sup>b</sup>Department of Materials Science and Engineering, Iowa State University, Ames, IA 50011, USA

<sup>c</sup>Center of Analysis and Testing, Wuhan University, Wuhan, China 430072

<sup>d</sup>Metals and Ceramics Division, Oak Ridge National Laboratory, Oak Ridge, TN 37831, USA

<sup>e</sup>Tata Institute of Fundamental Research, Bombay India 400005

<sup>f</sup>University of Missouri Research Reactor, Columbia, MO 65211, USA

Received 15 December 1999; accepted 28 April 2000

## Abstract

The equilibrium structural parameters, enthalpies of formation and partial densities of state for  $Ti_5Si_3$  and  $Ti_5Si_3Z_{0.5}$  ( $Z = B, C, N$  or  $O$ ) were calculated based on first-principle techniques. Enthalpy of formation calculations suggest that of the known structures for transition metal (TM) silicide compounds containing  $TM_5Si_3$  ( $D8_8$ ,  $D8_1$  and  $D8_m$ ) the  $D8_8$  structure is the most stable form of  $Ti_5Si_3$ , and the stability of the structure increases as  $Z$  atoms are added. The theoretically determined structural trends as a function of interstitial element,  $Z$ , agreed well with experimentally determined values. Both indicate bonding between  $Ti$  and  $Z$  atoms based on contraction of  $Ti-Z$  separations. The calculated partial densities of state suggest that  $p(Si)-d(Ti)$  and  $d(Ti)-d(Ti)$  interactions are responsible for most of the bonding in pure  $Ti_5Si_3$ , which agrees with previous studies. As  $Z$  atoms are added,  $p(Z)-d(Ti)$  interactions become significant at the expense of weakening some of the  $d(Ti)-d(Ti)$  interactions. © 2000 Elsevier Science Ltd. All rights reserved.

**Keywords:** A. Titanium silicides; B. Crystal chemistry of intermetallics; E. Electronic structure, calculation; F. Diffraction (electron, neutron and X-ray)

## 1. Introduction

Interest in  $M_5Si_3$  intermetallics ( $M =$  transition metal of groups III–VI) which began in the 1950's and continues today is primarily a result of their high melting points ( $> 2000^\circ C$ ), wide homogeneity ranges and large alloying potentials. Nowotny and coworkers performed much of the early characterization of these materials [1–3]. The crystal structures were determined to be either a hexagonal  $Mn_5Si_3$ -type ( $D8_8$ ,  $M = Sc, Ti, Mn, Y$ ), tetragonal  $Cr_5B_3$ -type ( $D8_1$ ,  $M = Cr, Nb, La, Ta$ ) or tetragonal  $W_5Si_3$ -type ( $D8_m$ ,  $M = V, Mo, W$ ). Additionally, Nowotny discovered that all of these  $M_5Si_3$  compounds, except  $La_5Si_3$ , reverted to the hexagonal form in the presence of boron, carbon, nitrogen, or oxygen [1].  $M_5X_3$  compounds stabilized in the hexagonal structure by ternary additions have since become known as Nowotny phases [2]. Experimental observations also suggested

that carbon was most efficient and oxygen least efficient in stabilizing the hexagonal structure. However, no direct experimental or theoretical evidence currently exists which explains why this stabilization occurs.

Although experimental evidence suggests that  $Ti_5Si_3$  does not require ternary additions to form the hexagonal structure, recent work has shown that small additions of carbon have a significant effect on the crystal structure, thermal expansion and high temperature oxidation resistance [4,5]. In fact, by adding carbon to the structure,  $Ti_5Si_3$  becomes a considerably more promising material for engineering applications [6,7] by reducing the anisotropy of thermal expansion and increasing oxidation resistance. However, little is known why carbon additions have such a striking effect on these properties. The goal of this study is to combine experimentally determined structural data with first-principle electronic calculations to understand bonding changes that occur with the addition of boron, carbon, nitrogen or oxygen to  $Ti_5Si_3$ . Determining these bonding changes will aid in

\* Corresponding author. Tel.: +1-515-294-0276.

understanding and predicting the changes that occur in the thermal and electronic properties.

No previous first-principle calculations have been attempted on ternary  $\text{Ti}_5\text{Si}_3\text{Z}_x$  ( $Z = \text{B}, \text{C}, \text{N}$  or  $\text{O}$ ); however, two studies do exist on binary  $\text{Ti}_5\text{Si}_3$ . The first study, by Long and Chong [8], used a semi-empirical tight binding energy band method with the extended Hückel approximation to calculate band structure and density of states (DOS). They concluded that bonding–antibonding in  $\text{Ti}_5\text{Si}_3$  is primarily a result of  $d(\text{Ti})$ – $p(\text{Si})$  interaction above and below the Fermi energy ( $E_f$ ) as well as  $d(\text{Ti})$ – $d(\text{Ti})$  interactions spanning energies around  $E_f$ . These orbital interactions are very typical of transition metal silicides in general and explain their good electrical conductivity [9,10]. The second study, by Ekman and Ozolins [11], made calculations based on the full potential version of the linear muffin tin orbital (LMTO) method. Their conclusions of  $d(\text{Ti})$ – $p(\text{Si})$  and  $d(\text{Ti})$ – $d(\text{Ti})$  hybridization were identical to those above. However, their electron density maps suggest that all Ti–Si interactions in  $\text{Ti}_5\text{Si}_3$  are multi-centered bonds as opposed to simple two-atom covalent bonds. The study also calculated the equilibrium volume, bulk modulus and enthalpy of formation, all of which were only slightly lower than the experimental values.

This study used the LMTO method with the atomic sphere approximation (ASA) to calculate the angular-momentum decomposed electronic DOS, but unlike the previous studies, equilibrium lattice parameters and atomic positions were also calculated. These calculations were made for  $\text{Ti}_5\text{Si}_3$ ,  $\text{Ti}_5\text{Si}_3\text{Z}_{0.25}$  and  $\text{Ti}_5\text{Si}_3\text{Z}_{0.5}$  ( $Z = \text{B}, \text{C}, \text{N}$  or  $\text{O}$ ) and compared to experimentally determined values. Heats of formation were also calculated for most compositions including  $\text{Ti}_5\text{Si}_3$  in the equilibrium  $\text{Mn}_5\text{Si}_3$  structure ( $D8_8$ ) as well as in the possible alternate structures of  $\text{W}_5\text{Si}_3$  ( $D8_m$ ) and  $\text{Cr}_5\text{B}_3$  ( $D8_1$ ).

## 2. Crystal structure of $\text{Ti}_5\text{Si}_3$

Fig. 1 gives the hexagonal structure of  $\text{Ti}_5\text{Si}_3$ . The unit cell contains two distinct titanium sites and one silicon site: Ti at 4d sites at  $(1/3, 2/3, 0)$ ; Ti at 6g sites at  $(x_{\text{Ti}}, 0, 1/4)$ ; Si at 6g sites at  $(x_{\text{Si}}, 0, 1/4)$ .

Theoretical calculations were based on this unit cell, which contains two formula units of atoms (i.e.  $\text{Ti}_{10}\text{Si}_6$ ). The  $\text{Ti}^{4d}$  atoms form a linear chain parallel to the  $c$ -axis, and the  $\text{Ti}^{6g}$  atoms form a chain of face-shared trigonal antiprisms along the  $c$ -axis. The silicon atoms form a chain of distorted face-shared trigonal antiprisms parallel to the  $c$ -axis such that one  $\text{Ti}^{4d}$  site is at the center of each antiprism. This structure leads to an ABAC stacking sequence along the  $c$ -direction. The B and C planes consist of  $\text{Ti}^{6g}$  and Si atoms, which form the shared faces of the antiprisms, and the A planes consist solely of  $\text{Ti}^{4d}$  atoms. The Z atoms are thought to occupy

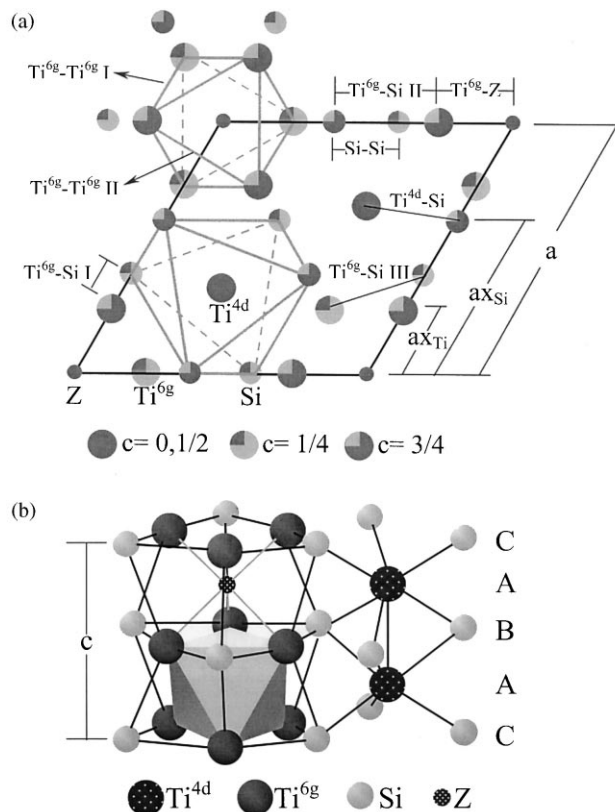


Fig. 1.  $D8_8$  crystal structure of  $\text{Ti}_5\text{Si}_3$ : (a) 001 orthographic projection of lattice with highlighted trigonal antiprisms; (b) depiction of the face-sharing of the trigonal antiprisms along the  $c$ -axis. Z atoms sit at the center of the trigonal antiprisms formed by six surrounding  $\text{Ti}^{6g}$  atoms.

the interstitial region at the center of the antiprism formed by the  $\text{Ti}^{6g}$  atoms, and hence, would also lie in the A plane with the  $\text{Ti}^{4d}$  atoms.

Strong experimental evidence exists to support the assertion that Z atoms occupy this interstitial site. Neutron diffraction studies of  $\text{Mo}_5\text{Si}_3\text{C}$  by Parthe et al. [3] and of  $\text{Ti}_5\text{Si}_3\text{H}_x$  by Kajitani et al. [12] as well as single crystal x-ray diffraction studies of  $\text{La}_5\text{Ge}_3\text{O}_x$  by Guloy and Corbett [13] and of  $\text{Er}_5\text{Si}_3\text{C}_x$  by Al-Shahery et al. [14] all agree that occupation of this antiprismatic interstice by Z atoms is most probable. Thus, the solubility of Z in  $\text{Ti}_5\text{Si}_3$  should vary from zero to the stoichiometric limit of  $\text{Ti}_5\text{Si}_3\text{Z}_1$  (there are only two antiprismatic interstices in the unit cell, which is equivalent to a maximum of one Z atom per formula unit). This is in full agreement with the actual solubility limits of C, N or O in  $\text{Ti}_5\text{Si}_3$  as measured by diffusion couple experiments [15,16].

## 3. Theoretical approach

Calculations to determine the stable structure were made within the local density approximation [17] by using the Hedin–Lundqvist [18] form for the local exchange and correlation potential. Electronic Bloch

states [19] were expanded as a mixed basis set with norm conserving scalar-relativistic pseudopotentials [20] used for the constituent elements. Relaxation of atomic coordinates was facilitated by computing the Hellmann–Feynman forces [21] acting on the atoms. A Broyden algorithm for estimating and updating this force matrix was used to predict the new atomic coordinates during the relaxation process. The atomic positions and lattice parameters were fully relaxed to the true equilibrium structure. Using these calculated equilibrium lattice parameters, electronic densities of state (DOS) were calculated by the LMTO-ASA method. To improve efficiency and accuracy of the calculations, unoccupied octahedral interstices were filled with empty spheres. For  $\text{Ti}_5\text{Si}_3$ , the radius of these spheres was set to 0.7 times the radius of the Ti atom. For  $\text{Ti}_5\text{Si}_3\text{Z}_x$ , the radius was set to the radius of the Z atom, which ranged from 0.68 to 0.7 times the radius of the Ti atom. Heats of formation were also calculated (see Section 5.1).

#### 4. Experimental approach

All  $\text{Ti}_5\text{Si}_3\text{Z}_x$  samples were synthesized by arc-melting. The starting materials included sponge titanium (Timet, 99.7%), silicon pieces (Alfa Aesar, 99.9999%), spectrographic grade graphite electrodes for carbon, boron pieces (Alfa Aesars, 99.5%), titanium nitride for nitrogen (Johnson Matthey, 99.8%) and titanium dioxide for oxygen (Fischer Scientific, 99.8%). Arc melting was done in a ultra-high-purity argon atmosphere on a water-chilled copper hearth. Samples were melted at least three times via a non-consumable tungsten electrode. Total weight losses after arc-melting were typically much less than 0.5 wt. %.

Arc-melted samples were then ground to  $< 20 \mu\text{m}$  and mixed with a silicon line position standard (NIST SRM 640b). Room temperature X-ray diffraction spectra were obtained from a Scintag diffractometer with solid state detector. Room temperature neutron diffraction spectra were obtained from the Missouri University Research Reactor (MURR) using a curved Ge monochromator and position sensitive detector. Rietveld analysis software (GSAS, Los Alamos National Laboratory, 1985) was used to calculate the lattice parameters and the two variable atomic coordinates,  $x_{\text{Ti}}$  and  $x_{\text{Si}}$ . Oxygen and nitrogen content were measured on a Leco TC-436 analyzer; carbon content was measured on a Horiba EMIA-520 analyzer.

#### 5. Results and discussion

##### 5.1. Enthalpy of formation

The enthalpies of formation were calculated from total energies,  $E$ , according to:  $H + E_{\text{Ti}_5\text{Si}_3\text{Z}_x} - \sum_i (X_i E_i)$ ,

where  $X_i$  is the concentration of the  $i$ th elemental component. The total energies of the elements,  $E_i$ , were calculated using their most stable structures: titanium (P6<sub>3</sub>/mmc), silicon (Fd-3m), boron (R-3m) and graphite (P6<sub>3</sub>/mmc), as well as O<sub>2</sub> and N<sub>2</sub> gas. For  $\text{Ti}_5\text{Si}_3\text{Z}_x$ , total energies,  $E_{\text{Ti}_5\text{Si}_3\text{Z}_x}$ , were calculated using the relaxed atomic positions and lattice parameters that were determined by the pseudopotential method described in Section 3.

Table 1 lists the results of these calculations. Of the three possible crystal structures in which  $\text{M}_5\text{Si}_3$  compounds form, the D8<sub>8</sub> structure has the largest negative value. Thus, these calculations agree with experimental observations that suggest that the D8<sub>8</sub> structure is the most stable structure for  $\text{Ti}_5\text{Si}_3$ . In most other  $\text{M}_5\text{Si}_3$  compounds, where M is heavier than Ti, the D8<sub>8</sub> structure only becomes favorable in the presence of interstitial atoms. As an example,  $\text{Mo}_5\text{Si}_3$ , which exists in the D8<sub>m</sub> structure, converts to the D8<sub>8</sub> structure when carbon is added. In a study by Fu et al. [22], calculations of enthalpies of formations did correctly suggest that in agreement with experimental evidence,  $\text{Mo}_5\text{Si}_3$  should form in the D8<sub>m</sub> structure instead of the D8<sub>8</sub> and D8<sub>1</sub> structures. Thus, this study provides further support that theoretical calculations of the enthalpy of formation can be used to predict which crystal structure is most stable.

As seen in Table 1, the enthalpy of formation becomes more negative, as more carbon or boron is added to the lattice. This suggests that these interstitial atoms, in accordance with experimental observations, do increase the stability of the D8<sub>8</sub> structure. A comparison of the enthalpy of formation of  $\text{Ti}_5\text{Si}_3$  with that of  $\text{Ti}_5\text{Si}_3\text{Z}_{0.5}$  indicate  $\text{Ti}_5\text{Si}_3\text{C}_{0.5}$  is 3% more negative,  $\text{Ti}_5\text{Si}_3\text{N}_{0.5}$  is 7% more negative and  $\text{Ti}_5\text{Si}_3\text{O}_{0.5}$  is 38% more negative than  $\text{Ti}_5\text{Si}_3$ . This trend agrees well with experimental values of the Gibbs energy of formation at 1100°C for  $\text{Ti}_5\text{Si}_3\text{Z}$ . As reported in Goldstein et al. [16],  $\text{Ti}_5\text{Si}_3\text{C}$  is 5% more negative,  $\text{Ti}_5\text{Si}_3\text{N}$  is 11% more negative and  $\text{Ti}_5\text{Si}_3\text{O}$  is 41% more negative than  $\text{Ti}_5\text{Si}_3$ .

##### 5.2. Equilibrium structural parameters

Theoretical and experimental structural parameters are given, respectively, in Tables 2 and 3. The theoretical

Table 1  
Calculated enthalpies of formation

Composition	Structure	Enthalpy, eV/f.u.
$\text{Ti}_5\text{Si}_3$	D8 <sub>1</sub>	−6.060
$\text{Ti}_5\text{Si}_3$	D8 <sub>m</sub>	−6.170
$\text{Ti}_5\text{Si}_3$	D8 <sub>8</sub>	−6.410
$\text{Ti}_5\text{Si}_3\text{B}_{0.25}$	D8 <sub>8</sub>	−6.604
$\text{Ti}_5\text{Si}_3\text{B}_{0.5}$	D8 <sub>8</sub>	−7.104
$\text{Ti}_5\text{Si}_3\text{C}_{0.25}$	D8 <sub>8</sub>	−6.625
$\text{Ti}_5\text{Si}_3\text{C}_{0.5}$	D8 <sub>8</sub>	−7.251
$\text{Ti}_5\text{Si}_3\text{N}_{0.5}$	D8 <sub>8</sub>	−6.866
$\text{Ti}_5\text{Si}_3\text{O}_{0.5}$	D8 <sub>8</sub>	−8.870

Table 2  
Calculated structural parameters for  $\text{Ti}_5\text{Si}_3\text{Z}_x^a$

$Z_x$	$a$ (Å)	$c$ (Å)	$x_{\text{Ti}}^a$	$x_{\text{Si}}^a$
–	7.377	5.084	0.2473	0.6063
$\text{B}_{0.25}$	7.4027	5.1079		
$\text{B}_{0.5}$	7.4101	5.1130	0.2470	0.6023
$\text{C}_{0.25}$	7.3775	5.0892		
$\text{C}_{0.5}$	7.3925	5.0956	0.2400	0.6023
$\text{N}_{0.25}$				
$\text{N}_{0.5}$	7.3834	5.0746	0.2410	0.6025
$\text{O}_{0.25}$				
$\text{O}_{0.5}$	7.3730	5.0829	0.2440	0.6025

<sup>a</sup> Values for the  $x$  coordinates of the 6g Ti ( $x_{\text{Ti}}$ ) and 6g Si ( $x_{\text{Si}}$ ) sites are in fractional units.

Table 3  
Measured structural parameters for  $\text{Ti}_5\text{Si}_3\text{Z}_x^a$

$Z_x$	$a$ (Å)	$c$ (Å)	$x_{\text{Ti}}^a$	$x_{\text{Si}}^a$
$\text{O}_{0.02}$	7.4601(1)	5.1510(1)	0.2507(3)	0.6067(2)
$\text{B}_{0.24}$	7.4670(2)	5.1722(2)	0.2495(3)	0.6076(5)
$\text{B}_{0.47}$	7.4781(1)	5.1788(1)	0.2478(3)	0.6053(5)
$\text{C}_{0.25}$	7.4497(1)	5.1596(1)	0.2446(3)	0.6032(2)
$\text{C}_{0.47}$	7.4415(1)	5.1687(1)	0.2391(3)	0.6004(2)
$\text{N}_{0.27}$	7.4387(1)	5.1453(1)	0.2439(2)	0.6049(3)
$\text{N}_{0.46}$	7.4273(1)	5.1543(1)	0.2379(3)	0.6025(5)
$\text{O}_{0.22}$	7.4469(2)	5.1410(1)	0.2454(2)	0.6041(2)
$\text{O}_{0.4}$	7.4342(1)	5.1334(1)	0.2419(2)	0.6015(2)

<sup>a</sup> Values for the  $x$  coordinates of the 6g Ti ( $x_{\text{Ti}}$ ) and 6g Si ( $x_{\text{Si}}$ ) sites are in fractional units.

lattice parameters underestimate the experimental lattice parameters by 0.6–1.6% as is common for this method of calculation. However, the normalized trends between experimental and theoretical values are in good qualitative agreement, particularly for the change in  $c$ -axis as a function of interstitial content. Boron and carbon, being the larger atoms, expand the “ $c$ ”-lattice parameter; whereas, the smaller oxygen and nitrogen contract it. The agreement between theoretical and experimental trends in the “ $a$ ”-lattice parameter is not quite as good. Based on experimental measurements, all but boron contract the “ $a$ ”-lattice parameter; although theoretical calculations show all but oxygen expand the “ $a$ ”-lattice parameter. The reason for this discrepancy may be due to the underestimation of the lattice by theoretical calculations, although additional research is necessary to confirm this assertion.

Based on the experimental and theoretical structural parameters, nearest-neighbor atomic separations were calculated in order to infer bonding changes as interstitial atoms are added to  $\text{Ti}_5\text{Si}_3$ . Fig. 2 shows the change in nearest-neighbor atomic separations as carbon is added to  $\text{Ti}_5\text{Si}_3$ . In general, all studied interstitial additions led to changes similar to those seen in Fig. 2. There is very good qualitative agreement between the experimental and theoretical changes in atomic separations as a function of interstitial content. The most striking effect of interstitial atoms is to contract the  $\text{Ti}^{6g}\text{-Ti}^{6g}$  and  $\text{Ti}^{6g}\text{-Z}$  separations and to expand the  $\text{Ti}^{6g}\text{-Si}$  separations. This suggests bonding between the

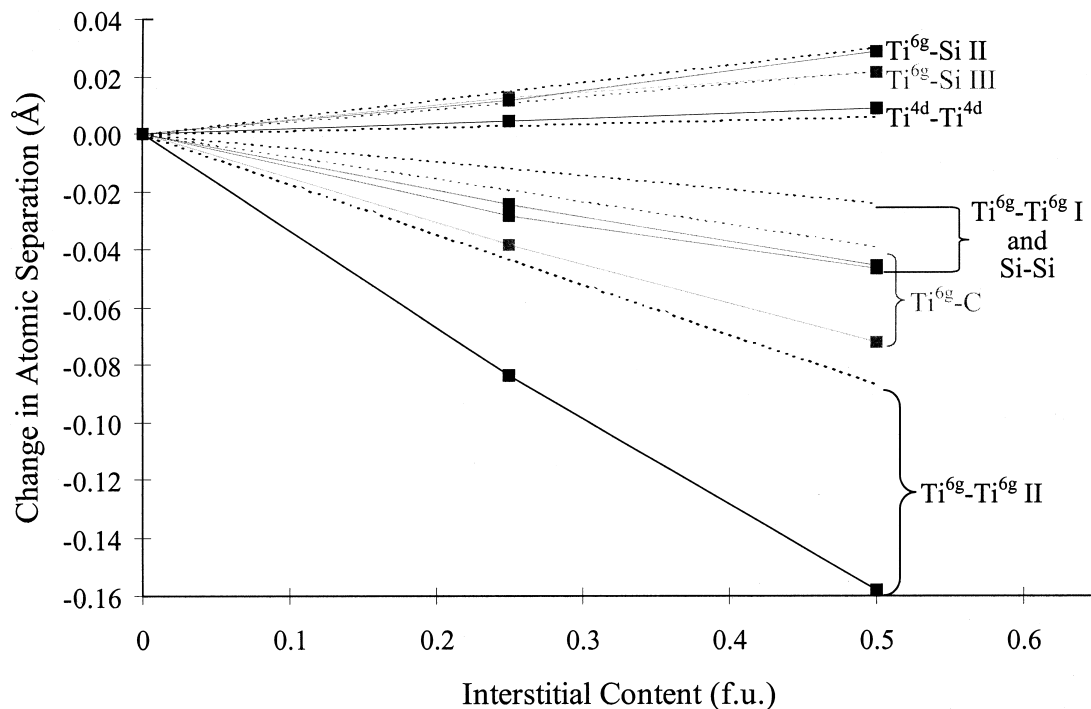


Fig. 2. Change in atomic separations as carbon is added to  $\text{Ti}_5\text{Si}_3$ . Dotted lines represent theoretical calculations, solid lines represent experimental data.

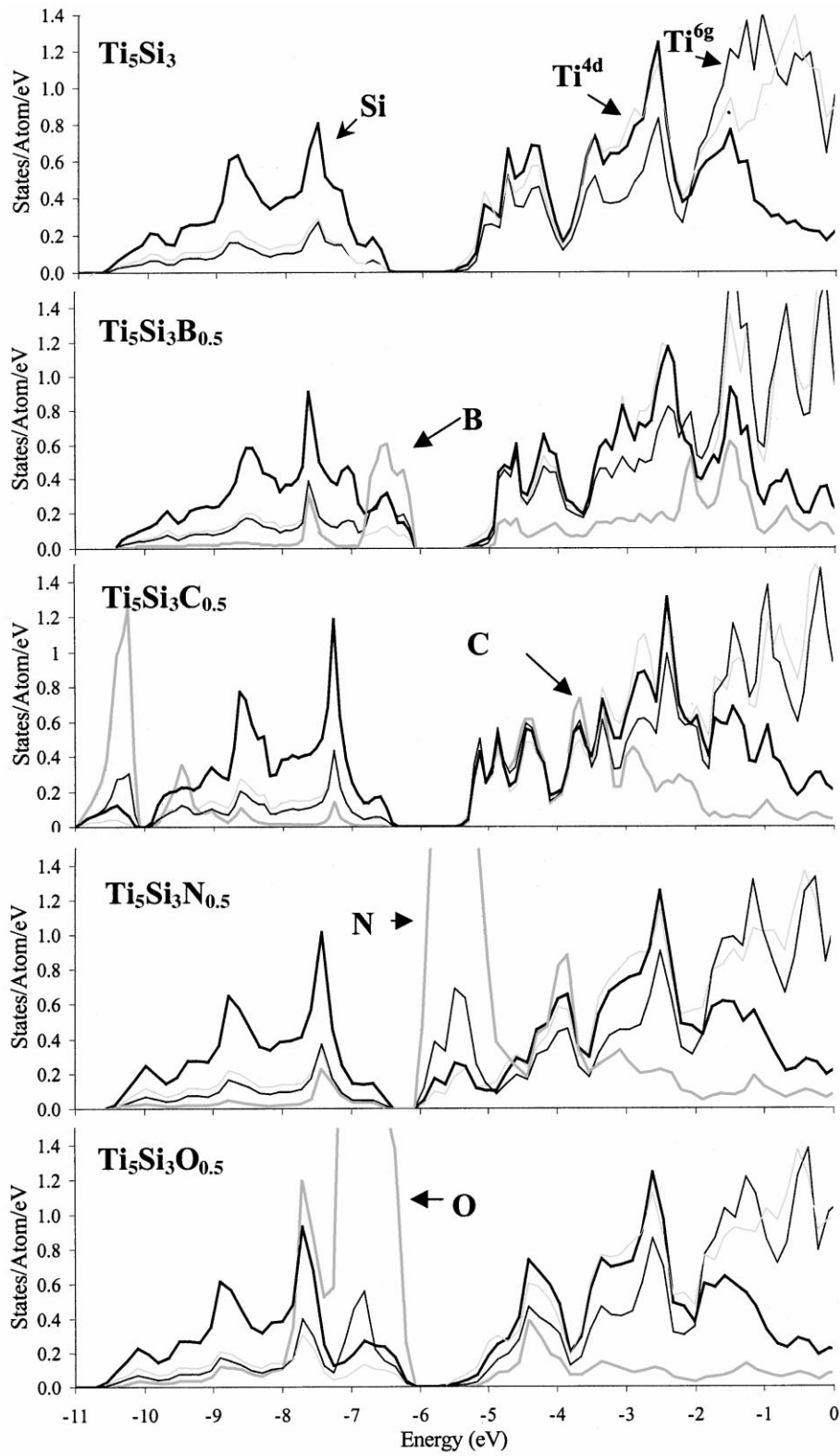


Fig. 3. PDOS's for  $\text{Ti}_5\text{Si}_3$  and  $\text{Ti}_5\text{Si}_3\text{Z}_{0.5}$ . Thick, black lines represent Si states; thick, grey lines are Z states; thin, black lines are  $\text{Ti}^{6g}$  states; thin, grey lines are  $\text{Ti}^{4d}$  states.

Ti<sup>6g</sup> and Z atoms and a possible weakening of bonding between the Ti<sup>6g</sup> and Si atoms. Furthermore, the theoretical calculations suggest that these changes are strongest for carbon. Thus, carbon atoms may be more strongly bonded with the Ti than the other interstitial atoms.

### 5.3. Densities of state

Fig. 3 gives the partial densities of state (PDOS's) for each of the atoms in Ti<sub>5</sub>Si<sub>3</sub> and Ti<sub>5</sub>Si<sub>3</sub>Z<sub>0.5</sub>. The calculated densities of state for Ti<sub>5</sub>Si<sub>3</sub> qualitatively agree with the previously mentioned studies by Long and Chong [8] and Ekman and Ozolins [11]; that is, the region from -2 to -5.5 eV is dominated by d(Ti)-p(Si) mixing, and the region at the Fermi level (0 eV) to -2 eV is dominated by d(Ti) states. These d(Ti) states most likely

consist of both bonding and non-bonding electrons. Also, little mixing occurs with the s(Si) states from -6.5 to -10.5 eV.

As boron, carbon, nitrogen or oxygen is added to the lattice, mixing occurs primarily between the interstitial atom's p-state and the surrounding Ti<sup>6g</sup> atom's d-state. This is shown in Fig. 4 for interstitial carbon and oxygen atoms, which is a plot of the cumulative area of the difference between the PDOS's of Ti<sub>5</sub>Si<sub>3</sub>Z<sub>0.5</sub> and Ti<sub>5</sub>Si<sub>3</sub>. A positive slope in Fig. 4 indicates an increase in the PDOS of an atom in Ti<sub>5</sub>Si<sub>3</sub>Z<sub>0.5</sub> compared to that same atom in Ti<sub>5</sub>Si<sub>3</sub>. Similarly, a negative slope indicates a decrease and a zero slope indicates no change in the PDOS's in Ti<sub>5</sub>Si<sub>3</sub>Z<sub>0.5</sub> relative to Ti<sub>5</sub>Si<sub>3</sub>. Thus, as seen in Fig. 4, addition of 0.5 formula units of oxygen leads to an increase of about 0.3 states for each Ti<sup>6g</sup> atom at -6 to -7 eV which corresponds exactly to the position of

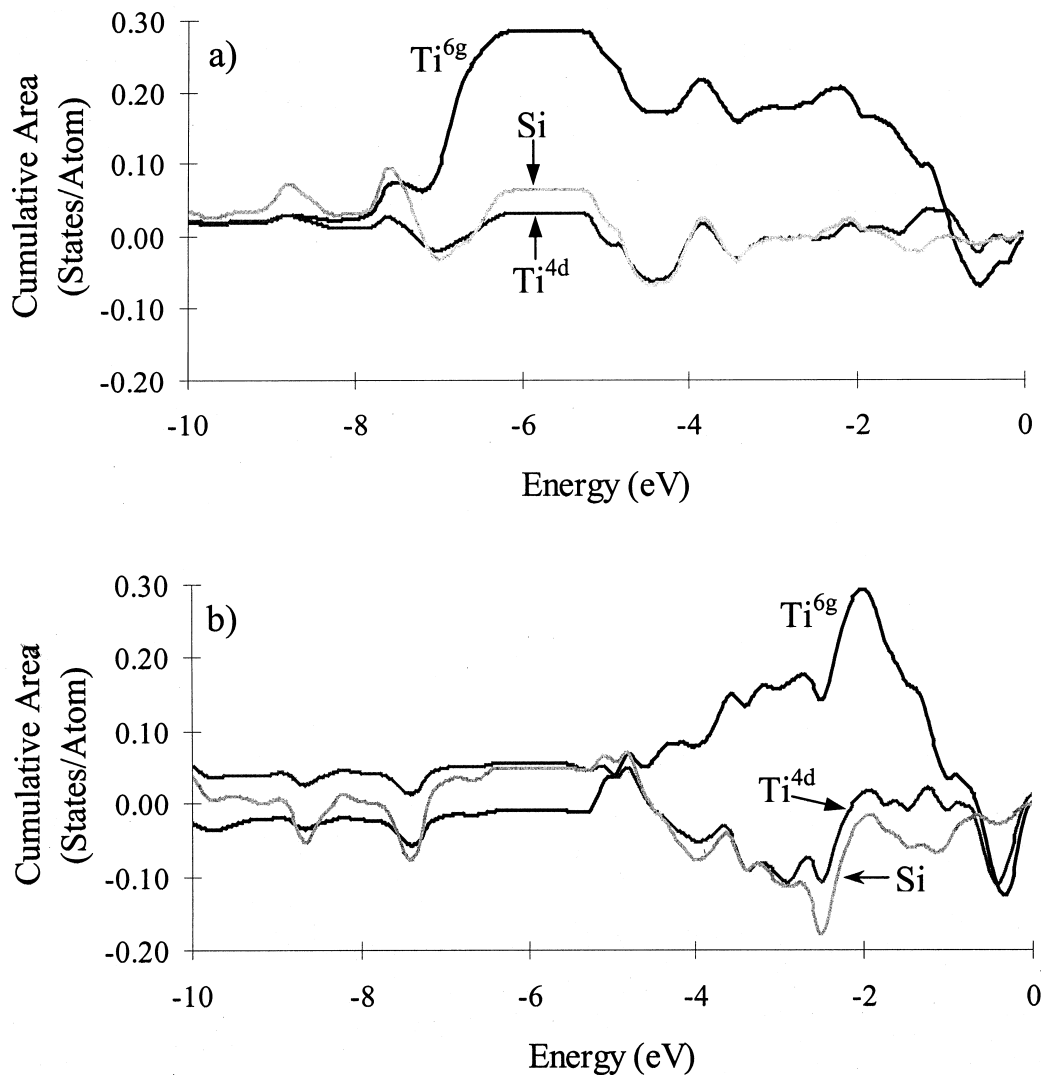


Fig. 4. (a) Cumulative area of the difference between the DOS of an atom of Ti<sub>5</sub>Si<sub>3</sub>O<sub>0.5</sub> and the DOS of that same atom in Ti<sub>5</sub>Si<sub>3</sub>. (b) Cumulative area of the difference between the DOS of an atom in Ti<sub>5</sub>Si<sub>3</sub>C<sub>0.5</sub> and the DOS of that same atom in Ti<sub>5</sub>Si<sub>3</sub>. Large, positive slopes in the Ti<sup>6g</sup> curves correspond exactly in energy to the position of the interstitial atom's p-state. Smaller features in these figures are due to slight changes in the Fermi level as interstitial atoms are added to Ti<sub>5</sub>Si<sub>3</sub>.

the oxygen p-band. Also, addition of oxygen leads to a reduction of 0.1 states per  $Ti^{6g}$  atom at  $-4.5$  to  $-5$  eV and a reduction of 0.25 states per atom at  $-0.5$  to  $-2$  eV which corresponds to areas of  $d(Ti)$ – $p(Si)$  and  $d(Ti)$ – $d(Ti)$  interaction, respectively.

Furthermore, little change occurs between the PDOS's of  $Ti^{4d}$  and Si atoms in  $Ti_5Si_3O_{0.5}$  relative to  $Ti_5Si_3$ . Based on these observations, addition of oxygen to  $Ti_5Si_3$  leads to the formation of  $d(Ti^{6g})$ – $p(O)$  bonds at the expense of  $d(Ti^{6g})$ – $d(Ti^{6g})$  interaction and to a lesser extent,  $d(Ti^{6g})$ – $p(Si)$  interaction. However,  $d(Ti^{4d})$ – $d(Ti^{4d})$  and  $d(Ti^{4d})$ – $p(Si)$  interactions remain relatively unaffected.

The effect of carbon addition is similar in that  $Ti^{6g}$  atoms show the most dramatic redistribution of electronic states. Also, the increase in states of the  $Ti^{6g}$  atoms coincides in energy with the carbon p-states ( $-2$  to  $-5$  eV) and the decrease in states of  $Ti^{6g}$  atoms coincides with states associated with  $d(Ti^{6g})$ – $d(Ti^{6g})$  interaction ( $-0.5$  to  $-2$  eV). However, unlike oxygen (and nitrogen), the carbon p-band is considerably broader and is located at similar energy levels as the Si p-band ( $-2$  to  $-5$  eV).

Although not shown, the effect of nitrogen additions is very similar to that of oxygen additions. Boron additions, however, leads to a redistribution of  $Ti^{6g}$  states around boron's s-band, which is located at  $-6$  to  $-7$  eV. The majority of boron's p-states are located at  $-1$  to  $-2$  eV, where  $d(Ti)$ – $d(Ti)$  interactions predominate.

Finally, although  $d(Ti^{6g})$ – $p(Z)$  bonding apparently forms at the expense of  $d(Ti^{6g})$ – $d(Ti^{6g})$  interactions, no significant change in DOS occurs at the Fermi level for all studied compositions. Also, although not obvious in Figs. 2 and 3, the overlap between  $Ti^{4d}$  and Si atoms increases slightly as interstitial atoms are added to  $Ti_5Si_3$ . This may suggest an increase in bonding between  $Ti^{4d}$  and Si atoms.

## 6. Conclusions

Based on enthalpy of formation calculations, the  $D8_8$  structure appears to be the most stable structure for  $Ti_5Si_3$  in accordance with experimental evidence. Also, interstitial additions appear to increase the stability of the  $D8_8$  structure. This increase in stability is apparently a result of bonding between the interstitial atom's p-electrons and the  $Ti^{6g}$  atom's d-electrons, which results in a strong contraction in separation between these atoms. These bonds form at the expense of  $Ti^{6g}$  states

located near the Fermi level. All other PDOS features remain relatively unaffected by the incorporation of interstitial atoms.

## Acknowledgements

Research at Ames Laboratory was contracted under contract No. W-7405-ENG-82 with the US Department of Energy by Iowa State University. Research at ORNL was sponsored by the Division of Materials Sciences, Office of Basic Energy Research, US Department of Energy under contract DE-AC05-96OR22464 with Lockheed Martin Energy Research Corporation. The work at MURR was supported by the US Department of Energy grant No. DE-FE02-90ER45427.

## References

- [1] Nowotny H, Lux B, Kudielka H. *Mh Chem* 1956;87:447.
- [2] Nowotny H. Electronic structure and alloy chemistry of the transition elements. In: Beck, PA editor. New York: Plenum Press, 1963. p.179.
- [3] Parthe E, Jeitschko W, Sadagopan V. *Acta Crystall* 1965;19:1031.
- [4] Thom AJ, Akinc M. *J Mater Sci Lett* 1994;13:1657.
- [5] Thom AJ, Akinc M. Advanced ceramics for structural and tribological applications. In: Hawthorne HM, Troczynski T, editors. Vancouver (BC): The Minerals, Metals & Materials Society, 1994. p.143.
- [6] Thom AJ, Young VG, Akinc M. *J of Alloys and Compounds* 2000;296:59–66.
- [7] Williams JJ, Kramer MJ, Malik SK, Akinc M. *J Mater Res* (in press).
- [8] Long X, Chong Z. *Trans Nonferrous Meta Soc China* 1994; 4(3):25.
- [9] Speier W, Kumar L, Sarma DD, de Groot RA, Fuggle JC. *J Phys: Condens Matter* 1989;1:9117.
- [10] Gelatt CD, Williams AR, Moruzzi VL. *Phys Rev B* 1983;27:2005.
- [11] Ekman M, Ozolins V. *Phys Rev B* 1998;57:4419.
- [12] Kajitani T, Kawase T, Yamada K, Hirabayashi M. *Trans Jpn Inst of Met* 1986;27(9):639.
- [13] Guloy AM, Corbett JD. *Inorg Chem* 1996;35:4669.
- [14] Al-Shahery GMY, Jones DW, McColm IJ, Steadman R. *J Less Common Metals* 1982;87:99.
- [15] Wakelkamp W. Diffusion and phase relations in the systems Ti–Si–C and Ti–Si–N. Thesis, Technical University of Eindhoven 1991.
- [16] Goldstein JI, Choi SK, Von Loo FJJ, Bastin GF, Metselarr R. *J Am Ceram Soc* 1995;78(2):313.
- [17] Jones RO. *Rev Mod Phys* 1989;61:689.
- [18] Hedin L, Lundqvist BI. *J Phys C* 1971;4:2064.
- [19] Louie SG, Ho KM, Cohen ML. *Phys Rev B* 1979;19:1774.
- [20] Hamann DR, Schluter M, Chiang C. *Phys Rev B* 1982;25:2103.
- [21] Ho KM, Elsasser C, Chan CT, Fahnle M. *J Phys: Condens Matter* 1992;4:5189.
- [22] Fu CL, Wang X, Ye YY, Ho KM. *Intermetallics* 1998;7:1.